

available at [www.sciencedirect.com](http://www.sciencedirect.com)journal homepage: [www.intl.elsevierhealth.com/journals/dema](http://www.intl.elsevierhealth.com/journals/dema)

# X-ray microcomputed tomography for measuring polymerization shrinkage of polymeric dental composites<sup>☆</sup>

Jirun Sun, Sheng Lin-Gibson<sup>\*</sup>

Polymers Division, National Institute of Standards and Technology, Gaithersburg, MD, USA

## ARTICLE INFO

### Article history:

Received 2 March 2007

Accepted 2 May 2007

### Keywords:

Dental materials

Image analysis

Polymerization shrinkage

Resin composites

X-ray microcomputed tomography

## ABSTRACT

**Objectives.** The main objective of this study was to assess the feasibility of using X-ray micro-computed tomography ( $\mu$ CT) as a viable technique for accurate measurements of composite volumetric changes due to polymerization.

**Methods.**  $\mu$ CT, a non-destructive 3D imaging technique that measures the intensity of content at each voxel, was used to determine the volume of experimental and commercial polymeric dental composites before and after photopolymerization. The experimental composites consisted of various mass ratios of 2,2-bis(4-(2-hydroxy-3-methacryloxypropoxy)-phenyl)propane (BisGMA) and triethylene glycol dimethacrylate (TEGDMA) filled with various amounts of barium boroaluminosilicate glass and fumed amorphous silica. Polymerization shrinkage was determined using  $\mu$ CT and shrinkage calculated based on density measurements.

**Results.**  $\mu$ CT was successfully used to calculate volumetric shrinkage of dental composites. Results agreed well with shrinkage obtained via density measurements of the same sample. The addition of radio opaque filler was necessary to achieve sufficient contrast between the sample and background. Appropriate image analysis procedures were needed to obtain the volumes of sample specimens.

**Significance.**  $\mu$ CT enables the characterization of polymerization shrinkage under clinically relevant conditions. In particular, the sample geometry and the physical state (liquid or solid) are flexible. The current test allowed multiple samples to be measured at the same time. In addition, the ability to accurately measure the size and shape of the object will allow multiple properties to be determined simultaneously.

© 2007 Academy of Dental Materials. Published by Elsevier Ltd. All rights reserved.

## 1. Introduction

While polymeric composites are being used increasingly as dental restoratives, volumetric contraction upon polymerization continues to be a major drawback [1–3]. In methacrylate based systems, the curing proceeds through the conversion of double bonds to single bonds, resulting in covalently bonded

monomers and a volumetric contraction [4]. The percentage of shrinkage depends on the chemical structure and relative molecular mass, filler content, and degree of conversion of the resin [5]. Polymerization shrinkage generates stress at the tooth/restorative interface and may lead to premature failures. The magnitude of stress and its distribution depend on the restoration size and the bonding geometry,

<sup>☆</sup> Official contribution of the National Institute of Standards and Technology; not subject to copyright in the United States.

<sup>\*</sup> Corresponding author at: 100 Bureau Drive, MS 8543, Gaithersburg, MD 20899-8543, USA. Tel.: +1 301 975 6765; fax: +1 301 975 4977.

E-mail address: [slgibson@nist.gov](mailto:slgibson@nist.gov) (S. Lin-Gibson).

0109-5641/\$ – see front matter © 2007 Academy of Dental Materials. Published by Elsevier Ltd. All rights reserved.

doi:10.1016/j.dental.2007.05.001

with the latter often characterized by the C-factor (ratio of bonded surface to free surface) [6]. With a strong emphasis on moving toward clinically relevant studies, methods for measuring polymerization shrinkage under controlled geometries is highly desirable but still lacking.

A number of methods have been developed to determine the polymerization shrinkage [4]. The most commonly used method is dilatometry [7], which measures volumetric changes of a material submersed in a liquid, usually mercury or water [8]. When performed under ideal conditions, shrinkage measurements obtained from a mercury dilatometer are generally accurate but arguably lacking in clinical relevance. Dilatometry is also laborious and time-consuming. Another limitation for mercury dilatometry is that it cannot be used to measure low viscosity flowable composites. Several other techniques, including the strain gauge, the bonded disk method, laser interferometry, and linometric techniques [8], measure changes in one dimension (linear shrinkage) which can then be converted to volumetric shrinkage. Results from these techniques often depend on the experimental setup as samples are typically confined in a defined geometry with different degrees of constraint. Other techniques including pycnometry and hydrostatic suspension have been applied to evaluate the volumetric changes based on density variations. The biggest drawback for all these techniques is their inability to examine shrinkage and dimensional changes simultaneously under clinically relevant conditions.

With the advent of X-ray microcomputed tomography ( $\mu$ CT), three-dimensional (3D) structures of small objects can be obtained with high spatial resolution [9,10].  $\mu$ CT inspects the internal structure of objects using a micro-focus X-ray source and collects the projected images by a planar X-ray detector. The object is rotated to allow multiple angular views to be acquired for reconstruction of an x–y slice. This procedure is carried out along different planes to generate 3D rendering of structures. Since  $\mu$ CT measures the object content in every voxel (the unit in 3D image analysis, analogous to the pixel in 2D image analysis), the precise volume of an object can be obtained.

$\mu$ CT has been widely accepted in biomedical research for examining bone [11,12] and tooth structures [13,14], and for visualizing structural features in tissue engineering scaffolds [15,16], among other applications.  $\mu$ CT has also been applied to assess the mineral concentration of teeth [17] and to study tooth macromorphology [18]. More recently,  $\mu$ CT has been used to analyze the structures at dentin–adhesive–composite interphase [19] and for evaluating 3D marginal adaptation [20]. In the latter work, the marginal adaptation was correlated with shrinkage strain obtained using the bonded disk method. An accurate assessment of the marginal adaptation depends on reliable volume calculations for the tooth and the restorative. The ability to accurately measure polymerization shrinkage coupled with marginal adaptation under clinically relevant setting would be ideal. However, a systematic investigation of  $\mu$ CTs ability to accurately determine the volume of restoratives or tooth structures has not been demonstrated.

In the current study, we conducted a systematic investigation into the use of  $\mu$ CT for determining the volumes of polymeric dental materials before and after photopolymerization and subsequently calculating the shrinkage. Multiple sets

of materials were examined to assess the robustness of the technique. In addition, detailed image analysis and its effect on the data accuracy and precision were explored.

## 2. Materials and methods

### 2.1. Materials<sup>1</sup>

Resins, 2,2-bis(4-(2-hydroxy-3-methacryloxypropoxy)phenyl)propane (BisGMA, density = 1.15 g/mL), and triethyleneglycol dimethacrylate (TEGDMA, density = 1.07 g/mL), were obtained from Esstech Inc. The photoinitiator system of camphorquinone (CQ) and ethyl 4-N,N-dimethylaminobenzoate (4E) was purchased from Aldrich Corp. The fillers, barium boroaluminosilicate glass (BBS, density = 2.0 g/mL) and fumed amorphous silica (OX50, density = 2.95 g/mL), were provided by the L.D. Caulk company. The average diameter for BBS and OX50 were 0.94  $\mu$ m and 0.04  $\mu$ m, respectively. Commercial composites A, B, and C, were Surefil (shade A) and TPH (shade A2) from Dentsply Caulk, and Filtek Supreme (shade A2) from 3M ESPE. All reagents were used as received.

### 2.2. Composite preparation

BisGMA and TEGDMA were mixed at several compositions. The resin mixtures were activated for blue light photopolymerization with 0.2% CQ and 0.8% 4E (by mass) and stored in the dark until use. The BBS and OX50 fillers were hand mixed into the activated resin until uniform. Two series of composites were prepared. The first series consisted of samples prepared with a constant BisGMA/TEGDMA mass ratio (50:50) and a varying amount of filler (BBS:OX50 = 9:1, filler loading = 8%, 20%, 30%, 40%, and 50%, by mass). Series two consisted of samples with constant filler loading (BBS:OX50 = 5:1, 30% by mass) and different BisGMA/TEGDMA resin compositions (70:30, 50:50, and 30:70 by mass).

### 2.3. X-ray microcomputed tomography

Each composite mixture (10–20 mg) was weighed and distributed into five polypropylene centrifuge tubes. All five tubes were placed in a sample holder for simultaneous  $\mu$ CT measurement. All samples were examined before and after photopolymerization using a Scanco Medical  $\mu$ CT 40 microcomputed tomography scanner. The micro-focus X-ray source was set to 70 kVp and 114  $\mu$ A. The samples were scanned at an 18  $\mu$ m resolution with an integration time of 300 s. After completion of the x–y scans, 250–450 slices were reconstructed and analyzed using the manufacturer's complete imaging and evaluation solution software.

All composites were cured using a Dentsply Triad 2000 visible light-curing unit with a tungsten halogen light bulb (250 W and 120 V). To ensure a high conversion, the sam-

<sup>1</sup> Certain equipment, instruments or materials are identified in this paper to adequately specify the experimental details. Such identification does not imply recommendation by the National Institute of Standards and Technology, nor does it imply the materials are necessary the best available for the purpose.

ples were cured for 5 min from the top and the bottom. Near infrared spectroscopy measured for composites with varying filler loading indicates that the degree of conversion was comparable regardless of the filler loading and is similar to the composites cured between glass slides. Shrinkage was calculated based on the volume difference evaluated using  $\mu$ CT,  $S_{\mu\text{CT}} = (V_1 - V_2)/V_1$ , where  $V_1$  and  $V_2$  were the volume of uncured and cured composite, respectively.

#### 2.4. Density measurements

The density of the uncured composites ( $\rho_1$ ) was calculated from the density of resins and fillers according to Eq. (1).

$$\rho_1 = \frac{1}{\sum_{i=1}^4 a_i/d_i} \quad (1)$$

where  $a_i$  and  $d_i$  are the mass fraction and density, respectively, of component  $i$ , where  $i$  includes the resins (BisGMA and TEGDMA) and fillers (BBS and OX50).

The density of the cured composites was obtained using a Sartorius YDK01 density determination kit. The mass of the cured composites was examined with a hydrostatic balance, which can determine the mass of a solid object in air as well as in water. Using Eq. (2), the specific density of the cured composites ( $\rho_2$ ) was determined.

$$\rho_2 = \frac{W_a \rho_{\text{fl}}}{W_a - W_{\text{fl}}} \quad (2)$$

where  $W_a$  is the mass of cured composites in air,  $W_{\text{fl}}$  the mass in water, and  $\rho_{\text{fl}}$  is the density of water. Distilled, deionized water was used. The density of water was adjusted according to the water temperature measured during the experiment. Using the above measurement, the volume of the cured composites can be calculated.

$$V_{\text{cal}} = \frac{W_a}{\rho_2} \quad (3)$$

Since the mass of the composites is conserved before and after curing, the shrinkage was derived by the density changes,  $S_p = (\rho_2 - \rho_1)/\rho_2$ .

#### 2.5. Statistical analysis

Polymerization shrinkage values calculated using  $\mu$ CT and density changes were analyzed statistically using analysis of variance (ANOVA) with a 95% confidence interval to indicate significant differences or lack thereof. The relative uncertainty associated with the volume calculations is approximated to be 5%.

### 3. Results and discussion

To assess the feasibility of  $\mu$ CT as a viable technique for routine characterization of polymerization shrinkage, the volumes of three series of composite samples before and after photopolymerization were examined. Series one and two were comprised of experimental samples with varying filler con-

tent and co-monomer composition, respectively. The resin is a binary mixture of commonly used dental monomers (BisGMA and TEGDMA). The filler phase is comprised of a mixture of BBS and OX50. BBS is a micron size filler often used to enhance the radio-opacity of the composites during X-ray radiographic analyses. The addition of BBS improves the contrast between the composites and the background in  $\mu$ CT measurements. OX50, a thixotropic filler with an average diameter of approximately 40 nm, was introduced to improve the suspension of the fillers in the resins. For the first two series of composites, the shrinkage is expected to change systematically, and these values can be compared with results obtained by other means. Series three included three commercial dental composites and was chosen to examine other factors that may affect the  $\mu$ CT results, including effects arising from chemical, physical, and processing parameters used during the commercial formulation. Most importantly, these three series of samples were designed to test the robustness of  $\mu$ CT for obtaining accurate volumes and subsequent shrinkage measurement of dental composites. In particular, we examined the ability of  $\mu$ CT to accurately quantify volumes for composites with varying radio-opaque filler content, a wide range of viscosities, and differing chemical compositions. While the same data processing and analysis was used throughout this study, the method validation, including threshold selection, volume calculation, and shrinkage evaluation, is discussed using data obtained from the first series of composites.

An accurate and precise volume for the composite before and after photopolymerization is necessary in order to acquire the correct shrinkage value. For  $\mu$ CT, the accuracy and precision of the volumes are highly dependent on the experimental design and subsequent image analysis. Accurate image analyses require a sufficient contrast between the object (composite) and background and the selection of appropriate segmentation values. For samples with filler content 8% (BBS content of 7.2%) and greater, the contrast between the composites and the background was adequate to allow clear separation. Composites with a lower BBS loading resulted in images with insufficient contrast between the composite and the background and, therefore, a large uncertainty in the volume calculation (data not shown).

The selection of appropriate segmentation values is critical in the image analysis. The segmentation converts 16 bit images into binary images and this procedure is particularly sensitive to the threshold value (i.e., voxel intensity below are background and voxel at or above the threshold intensity are considered sample). Fig. 1A shows a 16-bit image of a typical x-y slice which is converted into a binary image (Fig. 1B) upon the selection of an appropriate threshold value. Selection of a threshold greater or lower than the optimal value results in erroneous data conversion (Fig. 1C and D). Thus, an optimal threshold value must be used and we obtained this value according to Ridler's theory [21].

The threshold values for image analysis of the first series of composites before and after photopolymerization are illustrated in Fig. 2. The column graph shows the optimal threshold for each specimen before and after curing. Increasing the radio opaque BBS content increased the optimal threshold. As mentioned previously, the addition of BBS enhances X-ray contrast and therefore results in a larger threshold value. A compari-

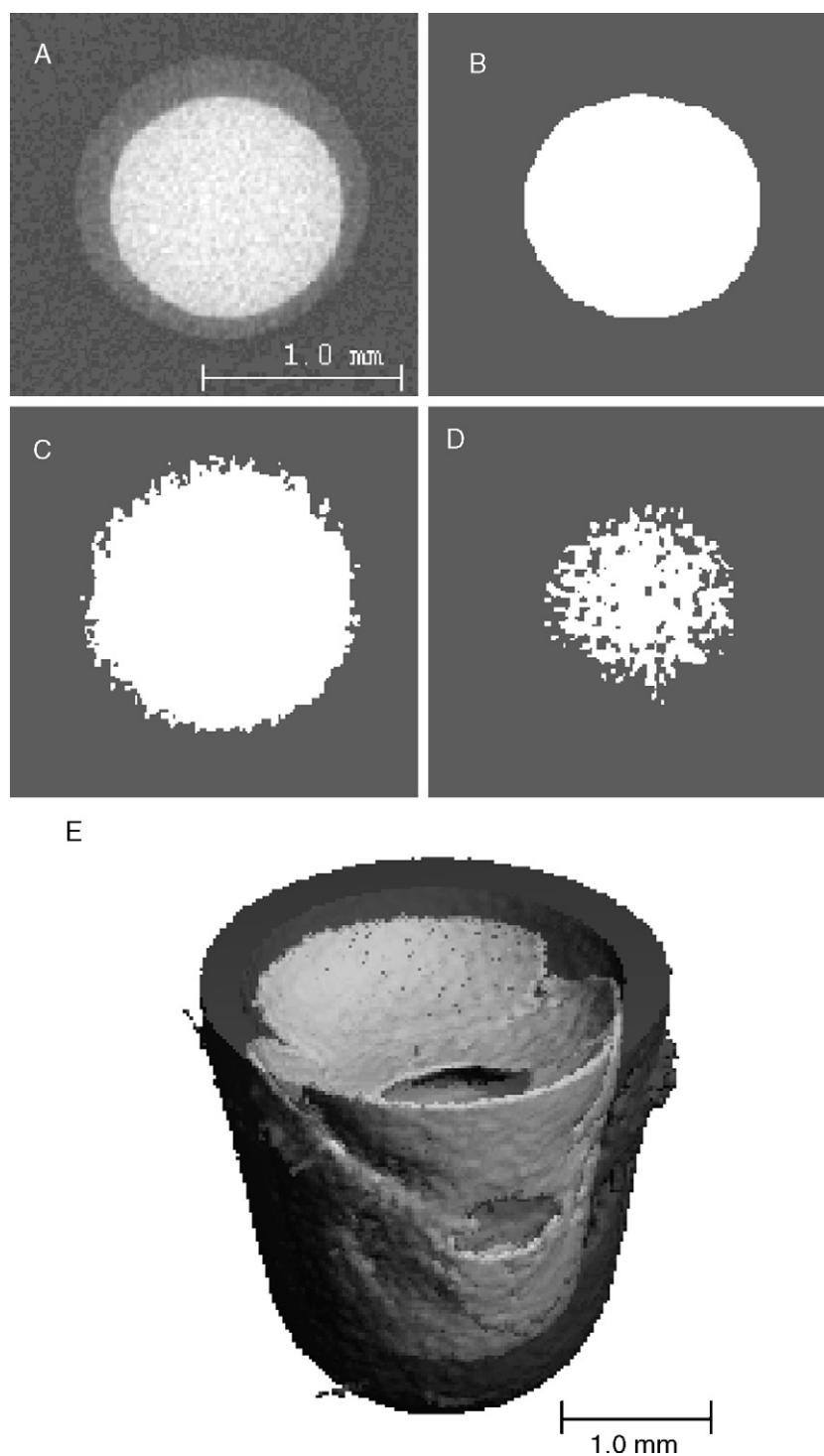


**Fig. 1 – One 2D slice and its analysis at different thresholds: (A) a typical 2D slice where the composite is in the lightest gray, the background in the darkest gray, and the polymer tube in the intermediate gray; (B) analysis of the composite at the optimal threshold; (C) analysis at a threshold lower than the optimal threshold; (D) analysis at a threshold greater than the optimal threshold; and (E) a 3D rendering of a composite specimen in a centrifuge tube. The composite is shown in light gray, the tube is shown in dark gray.**

son of the optimal threshold value for samples from the same batch measured at the same time reveals sample to sample variation. While the differences appear small, a slight deviation from the optimal threshold has a profound effect on

the volume calculated. Since the volumetric calculation is extremely sensitive to the threshold value, this indicates that an optimal threshold must be determined for each sample in order to obtain an accurate volume. The fluctuation of opti-

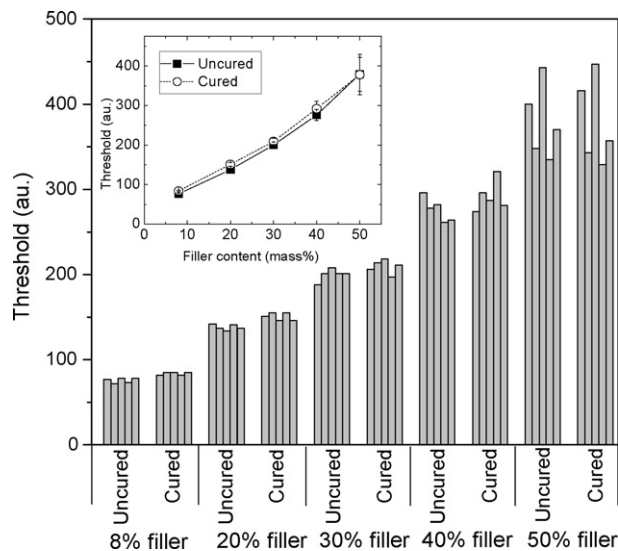


**Fig. 2 – Optimal thresholds at different filler contents (by mass) for composites in series one (columns). Five specimens of each composite were characterized before and after curing. The inset shows the average threshold for each composite (uncured and cured). The error bars represent the standard deviation and are an estimate of standard uncertainty. The lines through the data points are drawn to aid the reader's eyes.**

mal threshold among different specimens in the same group might be related to the sample inhomogeneities (different dispersion level of BBS), the sample geometry, the presence of air bubbles, and location of the sample with respect to the X-ray source. The inset of Fig. 2 plots the average threshold value for each uncured and cured composite. Application of the average optimal threshold value in place of each individually optimal threshold resulted in significantly larger uncertainties. The inset of Fig. 2 illustrates that the threshold value generally increased after polymerization, and this effect was more pronounced for composites with a lower filler loading. ANOVA revealed that threshold values are significantly different ( $p < 0.05$ ) for composites filled with 8% and 20% filler. A moderate increase in the threshold value upon polymerization for high shrinking materials is expected since the BBS density increased upon polymerization as the composite contracted.

Once the threshold was set, stacks of 2D images were compiled to reconstruct the 3D object, from which the composite volume was evaluated. A combined 3D image of a composite specimen in a centrifuge tube analyzed using two thresholds is illustrated in Fig. 1E. The composite is in light gray, which is evaluated at the optimal threshold of 85; the tube and composite is shown in dark gray and is obtained at a threshold of 30.

While using the optimal threshold produced the most consistent shrinkage results (highest precision), it was necessary to verify whether the volumes determined by  $\mu$ CT accurately reflected the actual volumes of the composites. To this end, volumes obtained from  $\mu$ CT were compared with those calculated from the weight and density of the cured composites (Eq. (3)). Table 1 lists results for the first series of composites with

**Table 1 – Volume validation for the same sample determined by  $\mu$ CT ( $V_{\mu\text{CT}}$ ) and density measurement ( $V_{\rho}$ ) for composites with varying filler content**

|  | Filler (% by mass) |      |      |       |       |
|--|--------------------|------|------|-------|-------|
|  | 8                  | 20   | 30   | 40    | 50    |
| $V_{\rho}$ (mm <sup>3</sup> )                    | 7.42               | 8.99 | 7.79 | 6.07  | 3.76  |
| $V_{\mu\text{CT}}$ (mm <sup>3</sup> )            | 7.40               | 9.01 | 7.87 | 5.92  | 3.70  |
| $V_{\mu\text{CT}} - V_{\rho}$ (mm <sup>3</sup> ) | −0.02              | 0.02 | 0.08 | −0.15 | −0.06 |
| Difference (%)                                   | −0.27              | 0.22 | 1.03 | −2.47 | −1.60 |

different filler loadings. The volumes obtained by these two independent measurements are consistent with each other, with deviations less than 2.5%. These results indicate that  $\mu$ CT can be used to accurately evaluate the volume of composites.

While the above results implied that the shrinkage can be obtained with good accuracy, we examined in detail the use of  $\mu$ CT for determining polymerization shrinkage. MicroCT was used to determine the polymerization shrinkage of three series of materials. The shrinkage ( $S_1$ ) was calculated based on the change of volume of composites before and after curing. Polymerization shrinkage results measured by  $\mu$ CT ( $S_1$ ) and density calculations ( $S_2$ ) for the first series of samples with varying filler content are illustrated in Fig. 3. Since the filler does not compress, the polymerization shrinkage is expected to increase as the filler content decreases. Results from the two measurements were consistent with each other and with the expected trend. Analyses using ANOVA showed no significant statistical difference between results obtained from  $\mu$ CT and density changes. The shrinkage values obtained from the density measurement had a larger standard deviation. The observed difference in the shrinkage values is in part due to the fact that the initial densities of gravimetric calculation were obtained from literature. Using the density values determined by  $\mu$ CT would bring the shrinkage values closer together.

The second series of composites were used to test the ability of  $\mu$ CT to characterize polymerization shrinkage of materials with varying chemical composition. The mass fraction of fillers in the composites was fixed at 30%. Bis-GMA (shrinkage  $\approx 6\%$ ) is the base monomer with a relatively high molecular mass and a rigid backbone, and therefore shrinks less than the lower molecular mass, flexible TEGDMA (shrinkage  $\approx 12\%$ ). Results from  $\mu$ CT were in accordance with the expected trend with compositions with higher TEGDMA concentration exhibiting higher polymerization shrinkage. The shrinkage values were  $(5.88 \pm 0.33)\%$ ,  $(7.32 \pm 0.23)\%$ , and  $(9.01 \pm 0.28)\%$  for BisGMA/TEGDMA mass fractions of 70:30, 50:50, and 30:70, respectively (Fig. 3B).

In the third series, three commercial composites (denoted as A, B, and C) were examined. These composites have fixed formulations and are broadly used as dental restoratives. The shrinkage values of these materials have been examined by different methods [22,7,23]. The shrinkage results from  $\mu$ CT and literature are listed in Table 2. Results obtained using  $\mu$ CT were generally within the range of the reported values. It should be noted that shrinkage values reported in literature have a broad range for each material due to differences in the polymerization technique (such as the use of



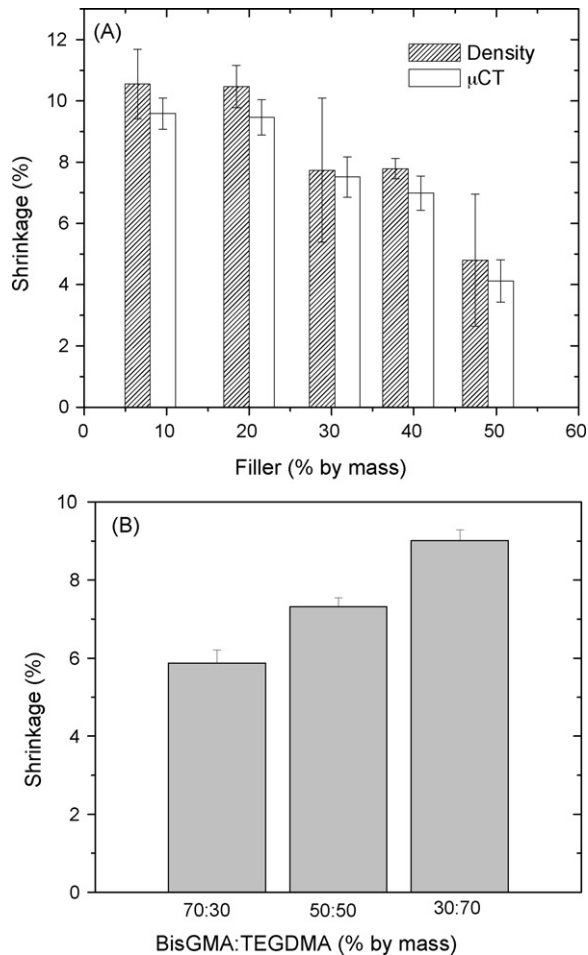


**Fig. 3 – (A) Polymerization shrinkage of composites with different filler contents determined by  $\mu$ CT and by density. (B) Polymerization shrinkage of composites with constant 30% filler and different TEGDMA to BisGMA ratios. The shrinkage was examined by  $\mu$ CT.**

different light source), degree of conversion, variations in the materials, and the measurement technique. Results obtained for this series of measurements indicate that  $\mu$ CT can be used to measure shrinkage in a broad range of commercial materials.

In addition to the advantages mentioned above,  $\mu$ CT can be used to examine samples of differing geometry and physical state (low viscosity liquids to solids). One prominent advantage of  $\mu$ CT over the other shrinkage measurement techniques is that  $\mu$ CT tolerates air bubbles entrapped within the sample. Because the volume is determined by calculating the volume of voxels separated from the background, the air bubbles are recognized as background and not counted in the volume of

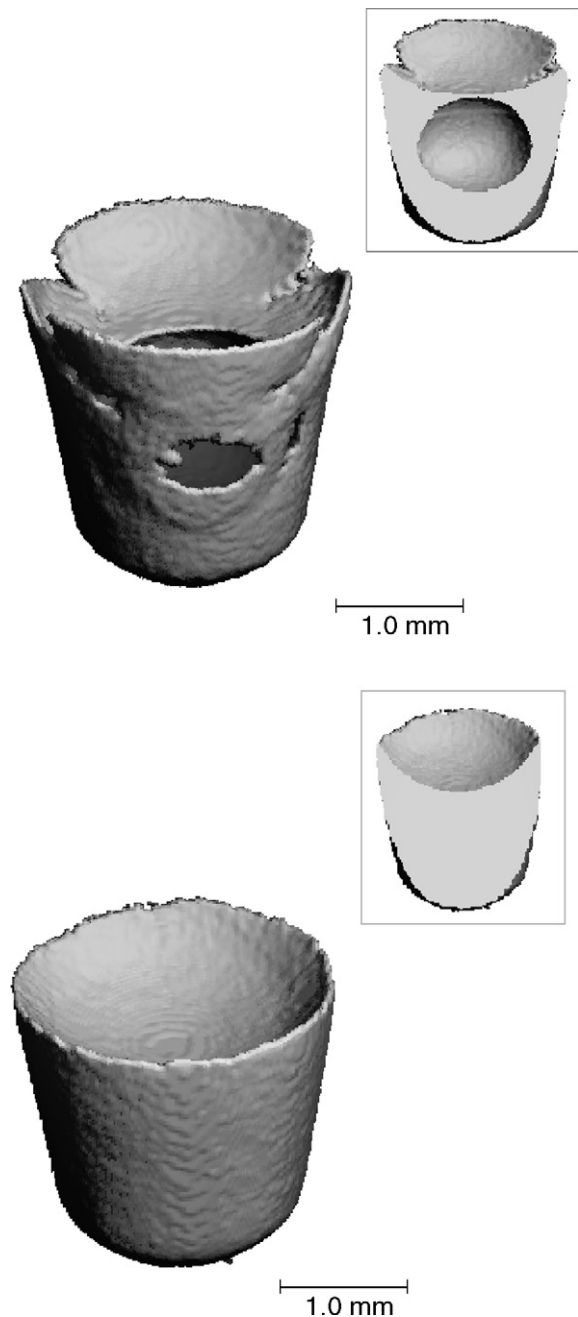


**Fig. 4 – Images generated by  $\mu$ CT, 3D view of one composite specimen before and after curing. Top image is from uncured composite, and the bottom image is from cured composite. Insets are the cut-plane view of the corresponding 3D image.**

composite. Two 3D images of a specimen (8% by mass filler content) from the first composite series generated by  $\mu$ CT are shown in Fig. 4, with Fig. 4A showing an uncured composite, and Fig. 4B showing the same composite after curing. The insets are cross-sections of the 3D images to illustrate the corresponding interior structure. Note that the uncured composite has a big air bubble, but its cured counterpart does not. The presence of entrapped air bubbles does not affect results obtained by  $\mu$ CT; however, it will most likely cause large errors

**Table 2 – Shrinkage of three commercial composites**

|                      | A               | B               | C               |
|----------------------|-----------------|-----------------|-----------------|
| $\mu$ CT results (%) | $1.07 \pm 0.09$ | $2.73 \pm 0.17$ | $2.49 \pm 0.18$ |
| Literature data (%)  | 0.8–1.4         | 1.6             | 2.31–2.46       |

for results obtained by other shrinkage measurement methods.

#### 4. Conclusion

The present study demonstrated that  $\mu$ CT can be used to effectively characterize the volume of polymeric dental composites before and after polymerization, thus allowing the determination of polymerization shrinkage. The utility of this method was validated on multiple experimental and commercial materials. The ability to characterize polymerization shrinkage using  $\mu$ CT overcomes typical measurement issues associated with shrinkage measurements.  $\mu$ CT tolerates air bubbles and provides the same accuracy for different shapes, and physical states (liquid or solid, high viscosity or low viscosity). Additionally,  $\mu$ CT enables measurement to be made on clinically relevant geometries by evaluating the volumetric shrinkage regardless of the degree of constraint. The variation of the shrinkage values is reasonable and acceptable.

#### Acknowledgements

The dental resins were kindly donated by Esstech Inc. We would also like to thank Drs. Joseph Antonucci and Nancy Lin for their technical assistance.

#### REFERENCES

- [1] Ernst CP, Meyer GR, Klocker K, Willershausen B. Determination of polymerization shrinkage stress by means of a photoelastic investigation. *Dent Mater* 2004;20:313–21.
- [2] Sakaguchi RL, Wiltbank BD, Murchison CF. Cure induced stresses and damage in particulate reinforced polymer matrix composites: a review of the scientific literature. *Dent Mater* 2005;21:43–6.
- [3] Dickensven SH, Takagi S, Chow LC, Bowen RL, Johnston AD, Dickens B. Physical and chemical-properties of resin-reinforced calcium-phosphate cements. *Dent Mater* 1994;10:100–6.
- [4] Jakubiak J, Linden LA. Contraction (shrinkage) in polymerization Part I. Fundamentals and measurements. *Polimery* 2001;46:522–8.
- [5] Tilbrook DA, Pearson GJ, Braden M, Coveney PV. Prediction of polymerization shrinkage using molecular modeling. *J Polym Sci Part B: Polym Phys* 2003;41:528–48.
- [6] Price RB, Derand T, Andreou P, Murphy D. The effect of two configuration factors, time, and thermal cycling on resin to dentin bond strengths. *Biomaterials* 2003;24:1013–21.
- [7] Oberholzer TG, Grobler SR, Pameijer CH, Rossouw RJ. A modified dilatometer for determining volumetric polymerization shrinkage of dental materials. *Meas Sci Technol* 2002;13:78–83.
- [8] Sakaguchi RL, Wiltbank BD, Shah NC. Critical configuration analysis of four methods for measuring polymerization shrinkage strain of composites. *Dent Mater* 2004;20:388–96.
- [9] Sharp LJ, Choi IB, Lee TE, Sy A, Suh BI. Volumetric shrinkage of composites using video-imaging. *J Dent* 2003;31:97–103.
- [10] Tiba A, Charlton DG, Vandewalle KS, Ragain JC. Comparison of two video-imaging instruments for measuring volumetric shrinkage of dental resin composites. *J Dent* 2005;33:757–63.
- [11] Kalender WA. X-ray computed tomography. *Phys Med Biol* 2006;51:R29–43.
- [12] Rueggeger P, Koller B, Muller R. A microtomographic system for the nondestructive evaluation of bone architecture. *Calcif Tissue Int* 1996;58:24–9.
- [13] Peters OA, Laib A, Rueggeger P, Barbakow F. Three-dimensional analysis of root canal geometry by high resolution computed tomography. *J Dent Res* 2000;79:1405–9.
- [14] Stock SR, Barss J, Dahl T, Veis A, Almer JD. X-ray absorption microtomography (microCT) and small beam diffraction mapping of sea urchin teeth. *J Struct Biol* 2002;139:1–12.
- [15] Landis FA, Stephens JS, Cooper JA, Cicerone MT, Lin-Gibson S. Tissue engineering scaffolds based on photocured dimethacrylate polymers for in vitro optical imaging. *Biomacromolecules* 2006;7:1751–7.
- [16] Ho ST, Huttmacher DW. A comparison of micro CT with other techniques used in the characterization of scaffolds. *Biomaterials* 2006;27:1362–76.
- [17] Clementino-Luedemann TN, Kunzelmann KH. Mineral concentration of natural human teeth by a commercial micro-CT. *Dent Mater J* 2006;25:113–9.
- [18] Plotino G, Grande NM, Pecci R, Bedini R, Pameijer CN, Somma F. Three-dimensional imaging using microcomputed tomography for studying tooth macromorphology. *J Am Dent Assoc* 2006;137:1555–61.
- [19] De Santis R, Mollica F, Prisco D, Rengo S, Ambrosio L, Nicolais L. A 3D analysis of mechanically stressed dentin-adhesive-composite interfaces using X-ray micro-CT. *Biomaterials* 2005;26:257–70.
- [20] Kakaboura A, Rahiotis C, Watts DC, Silikas N, Eliades G. 3D-marginal adaptation versus setting shrinkage in light-cured microhybrid resin composites. *Dent Mater* 2007;23:272–8.
- [21] Ridler TW, Calvard S. Picture thresholding using an iterative selection method. *IEEE Trans Syst Man Cybern* 1978;8:630–2.
- [22] Herrero AA, Yaman P, Dennison JB. Polymerization shrinkage and depth of cure of packable composites. *Quintessence Int* 2005;36:25–31.
- [23] Oberholzer TG, Pameijer CH, Grobler SR, Rossouw RJ. Volumetric polymerisation shrinkage of different dental restorative materials. *SADJ* 2004;59:8–12.